Protein Residues That Control the Reaction Trajectory in *S*-Adenosylmethionine Radical Enzymes: Mutagenesis of Asparagine 153 and Aspartate 155 in *Escherichia coli* Biotin Synthase[†]

Christine E. Farrar and Joseph T. Jarrett*

Department of Chemistry, University of Hawaii at Manoa, Honolulu, Hawaii 96822

Received December 11, 2008; Revised Manuscript Received February 5, 2009

ABSTRACT: Biotin synthase catalyzes the oxidative addition of a sulfur atom to dethiobiotin (DTB) to generate the biotin thiophane ring. This reaction is initiated by the reductive cleavage of the sulfonium center of *S*-adenosyl-L-methionine (AdoMet), generating methionine and a transient 5′-deoxyadenosyl radical that functions as an oxidant by abstracting hydrogen atoms from DTB. Biotin synthase contains a highly conserved sequence motif, YNHNLD, in which Asn153 and Asp155 form hydrogen bonds with the ribose hydroxyl groups of AdoMet. In the present work, we constructed four individual site-directed mutations to change each of these two residues in order to probe their role in the active site. We used molecular weight filtration assays to show that for most of the mutant enzymes binding of the substrates was only slightly affected. *In vitro* assays demonstrate that several of the mutant enzymes were able to reductively cleave AdoMet, but none were able to produce a significant amount of biotin. Several of the mutants, especially Asn153Ser, were able to produce high levels of the stable intermediate 9-mercapto-dethiobiotin. Some of the mutants, such as Asp155Asn and Asn153Ala, produced instead an alternate product tentatively identified by mass spectrometry as 5′-mercapto-5′-deoxyadenosine, generated by direct attack of the 5′-deoxyadenosyl radical on the [4Fe-4S]$^{2+}$ cluster. Collectively, these results suggest that the protein residues that form hydrogen bonds to AdoMet and DTB are important for retaining intermediates during the catalytic cycle and for targeting the reactivity of the 5′-deoxyadenosyl radical.

Biotin synthase (BioB)[1] is an AdoMet radical enzyme that catalyzes the final step in the biosynthesis of biotin, the oxidative addition of a sulfur atom between the C6 methylene and C9 methyl positions of DTB (*1, 2*). BioB binds AdoMet and DTB in an active site sandwiched between a catalytic [4Fe-4S]$^{2+}$ cluster and a sacrificial [2Fe-2S]$^{2+}$ cluster (Figure 1). The proposed reaction sequence is initiated by electron transfer through the [4Fe-4S]$^{2+}$ cluster into the AdoMet sulfonium, resulting in the reductive cleavage of AdoMet into methionine and a transient high-energy 5′-deoxyadenosyl radical (Figure 2). This radical then abstracts a hydrogen atom from the C9 methyl of dethiobiotin (*3*), generating a dethiobiotinyl carbon radical that is quenched by a *μ*-sulfide from the [2Fe-2S]$^{2+}$ cluster (*4*), generating 9-mercaptode-thiobiotin (9-MDTB) as a discrete intermediate (*5*). A similar reaction sequence with a second equivalent of AdoMet results in abstraction of a hydrogen atom from the C6 methylene of 9-MDTB, and the resulting carbon radical is quench via
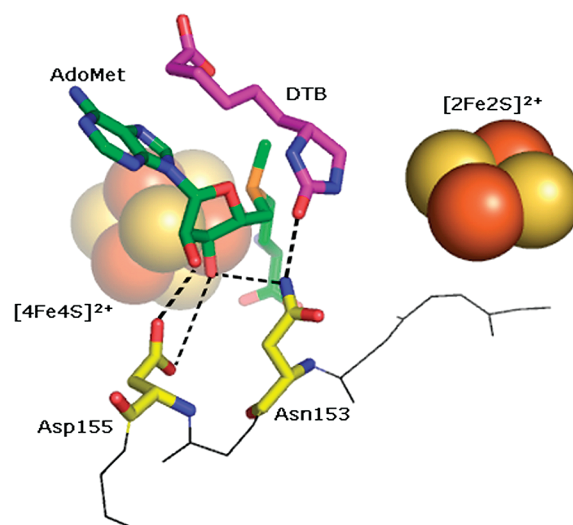

FIGURE 1: Structure of the active site of *E. coli* BioB showing the relative positioning of AdoMet (green) and DTB (pink) with respect to the [4Fe-4S]$^{2+}$ and [2Fe-2S]$^{2+}$ clusters. Asn153 and Asp155 form hydrogen bonds to the AdoMet ribose hydroxyl groups and may contribute to the positioning of this substrate.

intramolecular C−S bond formation to generate the biotin thiophane ring (*3*).

Biotin synthase is a member of the "radical SAM" superfamily of enzymes that is largely defined by a consensus CxxxCxxC sequence that binds the [4Fe-4S]$^{2+}$ cluster (*6, 7*). While all enzymes in this superfamily bind AdoMet, the

[1] Abbreviations: AdoMet, *S*-adenosyl-L-methionine; BioB, biotin synthase; 5′-dAH, 5′-deoxyadenosine; 5′-dA•, 5′-deoxyadenosyl radical; DTB, dethiobiotin; DMPD, *N,N*-dimethyl-*p*-phenylenediamine; DTT, dithiothreitol; ESI MS, electrospray ionization mass spectrometry; 5′-MdAH, 5′-mercapto-5′-deoxyadenosine; 9-MDTB, 9-mercaptodethio-biotin; Tris, tris(hydroxymethyl)aminomethane.
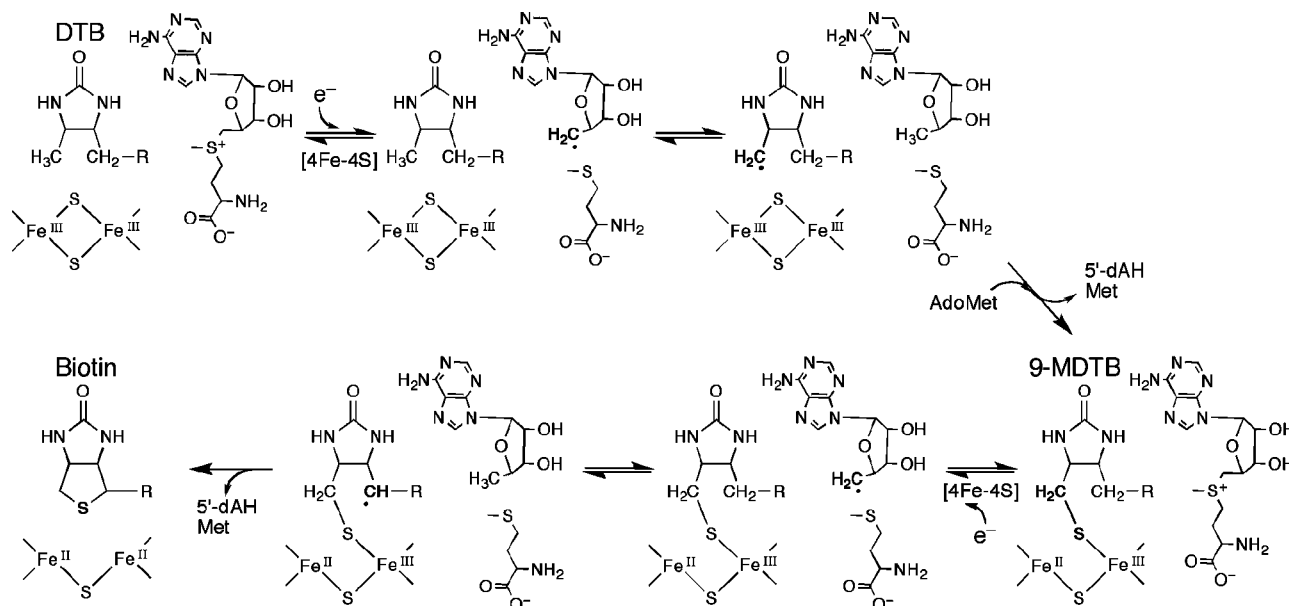
FIGURE 2: Proposed reaction sequence catalyzed by BioB. Two rounds of reductive cleavage of AdoMet are coupled to the abstraction of two hydrogen atoms from DTB, leading to the formation of two new C−S bonds. In the first half-reaction (top), following reductive cleavage and hydrogen abstraction, a dethiobiotinyl carbon radical is quenched through formation of a new C−S bond between DTB and a μ-sulfide of the $[2Fe-2S]^{2+}$ cluster. The second round of reductive cleavage and hydrogen abstraction (bottom) leads to completion of the thiophane ring and destruction of the $[2Fe-2S]^{2+}$ cluster. 9-MDTB is formed as a stable intermediate.

residues contacting the AdoMet are not universally conserved (*8*). However, conservation of these residues is high among a subset of these enzymes that includes BioB and LipA (*8*). These semiconserved motifs are "Y[150]NHNLD" in *Escherichia coli* BioB and "F[191]NHNLE" in *E. coli* LipA. Asp155 is involved in hydrogen bonds to both the 2′- and 3′-hydroxyl groups of the AdoMet ribose (Figure 1), and it is likely that the corresponding glutamate has a similar role in LipA (*8*). In contrast, while Asn153 of BioB is involved in hydrogen bonds with both the AdoMet 3′-hydroxyl and the dethiobiotin ureido ring (Figure 1), the LipA substrate, octanoyl-E2/H protein, has no hydrogen-bonding capability near the site of sulfur insertion. It therefore seems likely that these residues are preserved for reasons other than simple substrate binding. Nicolet and Drennan propose that these common residues may be involved in orienting 5′-dA• for abstraction of hydrogen atoms in similar reaction sequences (*8*). In addition, an examination of the structures of coproporphyrinogen III synthase (HemN) (*9*), molybdopterin precursor Z synthase (MoaA) (*10*), and lysine-2,3-aminomutase (KamA) (*11*), less homologous AdoMet radical enzymes that do not share the BioB/LipA motif, reveals that similar hydrophilic groups form hydrogen bonds to the AdoMet ribose hydroxyl groups: Asp209 and Gln172 in HemN, Ser126 and Asn165 in MoaA, and the AdoMet carboxylate and the Gln258 backbone amide in KamA. This functional conservation suggests that the carboxylate and carboxamide groups may play an important role in modulating and guiding AdoMet and/or 5′-dA• reactivity.

The mechanisms of many AdoMet radical enzymes can be written such that there is essentially no direct involvement of the protein beyond providing a scaffold that promotes close proximity of substrates and FeS clusters. Little is known regarding the more subtle question of how AdoMet radical enzymes promote the production of the 5′-dA• radical and also control the reactivity of this powerful oxidant. In BioB, the proximity of the conserved YNHNLD motif, and in

particular Asn153 and Asp155, to both AdoMet and DTB has led to speculation that these residues play a significant catalytic role. One recent study by Lotierzo et al. investigated the role of these residues by mutagenesis (*12*). They showed that when Asn153 and Asp155 were replaced by alanine, the enzymes were still able to bind both FeS clusters and had spectroscopic properties similar to those of WT enzyme. While they did not conduct substrate-binding studies, they did report that the EPR spectrum of the $[4Fe-4S]^+$ cluster in each mutant protein was modified by the addition of AdoMet and DTB, suggesting probable binding of the substrates to the mutant proteins. However, they did not observe any biotin production by their mutants, nor did they detect products of the reductive cleavage of AdoMet. Lotierzo et al. proposed that Asn153 and Asp155 may play a role in modulating the reactivity of AdoMet and/or that removal of these hydrogen bonds in the active site could potentially change the redox properties of the FeS clusters.

We propose at least three possible roles for these residues: (i) energetic contributions to the binding energy for AdoMet and/or DTB, (ii) positioning of AdoMet relative to the $[4Fe-4S]^{2+}$ cluster to promote the initial reductive cleavage of the sulfonium, or (iii) positioning the 5′-dA• radical with respect to DTB to promote hydrogen atom abstraction. To further probe how the reactivity of AdoMet is tuned and controlled by Asn153 and Asp155, we substituted each residue with other amino acids capable of hydrogen bonding to the ribose but with slightly different steric restrictions: Asn153 was changed to Asp, Gln, Ser, and Ala, and Asp155 was changed to Asn, Glu, Ser, and Ala. In addition, we examined the double mutant Asn153Ala/Asp155Ala. A careful characterization of the reactivity of these mutants using HPLC and ESI MS reveals that most of these mutants have some catalytic activity, but this reactivity does not lead to the production of significant amounts of biotin. Instead, we detect alternate products that suggest difficulty in controlling the subsequent radical chemistry. In particular, we detect 5′-

mercapto-5′-deoxyadenosine as a novel alternate byproduct of the AdoMet reductive cleavage reaction that is present in all samples, including WT enzyme, but is significantly increased in several mutants.

MATERIALS AND METHODS

Materials. All reagents were purchased from commercial sources and used without further purification. AdoMet was purchased as the *p*-toluenesulfonate salt and contains <5% 5′-methylthioadenosine and <1% *S*-adenosyl-L-homocysteine contamination. The concentration of AdoMet and 5′-dAH were determined using $\epsilon_{260} = 15400 \text{ M}^{-1} \text{ cm}^{-1}$. Synthetic 9-MDTB disulfide and (²H-9-*methyl*)-DTB were gifts from Prof. Andrée Marquet (Université Paris) and were synthesized according to published procedures (*3, 13*). His₆-BioB was prepared as previously described (*14*), and the N-terminal hexahistidine tag was not removed. The concentration of aerobically purified BioB was estimated based on the absorbance spectrum of the $[2Fe\text{-}2S]^{2+}$ cluster using $\epsilon_{452} = 8400 \text{ M}^{-1} \text{ cm}^{-1}$.

Site-Directed Mutagenesis. BioB mutants were constructed by the QuickChange method (Stratagene) using WT plasmid pJJ15-4A as a template (*14*) and PCR primers (Integrated DNA Technologies) that overlap the Asn153 and Asp155 codons. The mutated plasmids were isolated from strain DH5α, and the entire BioB gene was confirmed by sequencing. The isolated plasmids were transformed into strain BL21(DE3)pLysS (Novagen), and the mutant proteins were expressed and purified as previously described for WT enzyme (*14*).

Iron and Sulfur Analysis. Samples of WT and mutant proteins were diluted to approximately 0.5 mM in 50 mM Tris-HCl (pH 8.0). Accurate protein concentration was then determined using the Bradford assay with a commercial BSA standard (Bio-Rad). Protein concentrations were divided by a correction factor of 1.10, previously determined by quantitative amino acid analysis of the WT protein (*15*). The mutant protein samples were then subjected to iron analysis with bathophenanthroline (*16, 17*) and sulfide analysis with *N,N*-dimethyl-*p*-phenylenediamine (*18, 19*) using previously described modified methods (*15*), with ratios reported representing the average and standard deviation for three samples.

Substrate and Product Binding Assay. A filtration binding assay using 10 kDa centrifugal concentrators as filters was employed to measure the binding of substrates and reaction products to BioB. The amount of substrate bound to WT and mutant BioB proteins was determined for samples (500 μL) that had been incubated with substrates only (without flavodoxin, ferredoxin (flavodoxin):NADP⁺ oxidoreductase, or NADPH) for 30 min at room temperature. The amount of product bound to WT and mutant BioB proteins was determined for samples (500 μL) that had been incubated under normal assay conditions (see below) for 120 min at 37 °C. All experiments were carried out under anaerobic conditions in a nitrogen glovebox. Protein samples (100 μM) were incubated with FeCl₃ (6 equiv), Na₂S (6 equiv), and DTT (5 mM) in 50 mM Tris-HCl, pH 8.0, for 10 min to reconstitute the $[4Fe\text{-}4S]^{2+}$ cluster, and then varying concentrations of AdoMet and DTB were added. A small sample (70 μL) was removed by syringe; this sample was used to

determine the total (bound + free) DTB, AdoMet, or product in the assay mixture. The remainder of the assay solution was transferred to a 0.5 mL Microcon 10 kDa centrifugal concentrator, and a portion of the sample was filtered by centrifugation at 6000*g* for 2 min. The filtrate was used to determine the free DTB, AdoMet, or product in the assay mixture. Each sample (70 μL) was then acidified to precipitate the protein by addition of 4.5 M sodium acetate, pH 4.5 (3.5 μL), the acidified samples were clarified by centrifugation at 18000*g* for 10 min, and the supernatant was analyzed by HPLC as described for the activity assay. Commercial dethiobiotin, AdoMet, or biotin samples (100 μM) analyzed on the same day were used as external standards. The peak area measured for unknown samples of product and alternate products was converted to concentration using the peak area measured for the biotin, dethiobiotin, or AdoMet standards. The difference between the initial sample (total substrate or product) and the filtrate (free substrate or product) was used to calculate the fraction of substrate bound. The fraction bound can also be calculated directly from the ratio of peak areas without standards. Control samples that contained only substrates or products in the same buffers, but with no protein components, demonstrated that <2% of these compounds are lost due to binding to the plastic or filter in the centrifugal concentrator.

Activity Assay. Biotin synthase (25−100 μM in 200 μL final volume) was added to septum-covered vials containing 50 mM Tris-HCl, 100 mM KCl, and 5 mM DTT, pH 8.0, and degassed under argon. The $[4Fe\text{-}4S]^{2+}$ cluster was reconstituted by incubation with 4 equiv each of Na₂S and FeCl₃ for 5 min. Flavodoxin (25 μM), ferredoxin (flavodoxin):NADP⁺ oxidoreductase (4 μM), NADPH (1 mM), and AdoMet (1−5 equiv) were added while the vials were continuously degassed. Turnover was initiated by addition of DTB (1−5 equiv), and the vials were incubated in a 37 °C water bath for 5−360 min. Acetic acid/sodium acetate, pH 4.5 (20 μL of 4.5 M stock), was added to quench the reaction and precipitate the protein. The vials were incubated on ice to ensure full precipitation, the precipitate was removed by centrifugation for 10 min at 18000*g*, and the supernatant was transferred to an HPLC autosampler vial. For analysis of DTB, biotin, and alternate products (gradient I), samples were injected on a Waters Atlantis dC18 reversed-phase column (3.0 × 150 mm, 5 μm) and eluted with a 25 min linear gradient from 2% to 25% acetonitrile in H₂O containing 0.1% H₃PO₄ at a flow rate of 1 mL/min and a column temperature of 35 °C. DTB ($t_R = 22$ min), 9-MDTB ($t_R = 24$ min), and biotin ($t_R = 18$ min) were detected using UV absorbance at 210 nm. For analysis of 5′-deoxyadenosine, AdoMet, and alternate products (gradient II), samples were injected on a Waters Atlantis dC18 reversed-phase column (3.0 × 150 mm, 5 μm) and eluted with a 30 min linear gradient from 2% to 15% buffer B (buffer A, 50 mM NaH₂PO₄, 10 mM heptanesulfonic acid, 4% acetonitrile, pH 2.0; buffer B, 90% acetonitrile in H₂O) at a flow rate of 1 mL/min and a column temperature of 25 °C. 5′-Deoxyadenosine ($t_R = 12$ min) and AdoMet ($t_R = 23$ min) were detected at 260 nm. Fresh external standards containing biotin, DTB, AdoMet, and 5′-deoxyadenosine (10−250 μM) were prepared and analyzed prior to and following each set of samples to ensure accurate identification and quantitation. 9-MDTB was quantified by comparison to the integration

of an external biotin standard, assuming that 9-MDTB has an identical extinction coefficient as biotin.

Mass Spectrometry. The mass of BioB reaction products was determined by high-pressure liquid chromatography with electrospray-ionization mass spectrometry detection (HPLC ESI MS). Chromatographic separation was performed on an Agilent 1100 series liquid chromatography system (Agilent Technologies) equipped with an Eclipse XDB-C18 column (4.6 mm × 150 mm, 5 μm, Agilent) using a 25 min linear gradient from 95:5 to 70:30 H_2O:acetonitrile (both containing 0.1% (v/v) formic acid) at a flow rate of 0.7 mL/min. The LC system was coupled to an Agilent 6210 time-of-flight mass spectrometer equipped with an electrospray ionization source operating in positive ion mode. Nitrogen was used as the nebulizer drying gas (pressure, 30 psi; flow rate, 7 L/min; temperature, 350 °C). Additional ESI MS parameters were as follows: spray capillary voltage, 3500 V; skimmer voltage, 65 V; fragmenter voltage, 175 V; OctRFV voltage, 250 V. Mass spectra were acquired over the range $m/z =$ 150−1000 at a scan speed of 0.99 scan/s. Agilent MassHunter workstation software (v B.01.03, Agilent) was used for instrument control, data acquisition, and data analysis.

RESULTS

Site-Directed Mutagenesis of Asn153 and Asp155 in BioB. The structure of *E. coli* BioB shows that the conserved motif Y[150]NHNLD is contained within a β-strand that spans the length of the active site (*20*). However, only Asn153 and Asp155 contact the substrates: Asn153 forms hydrogen bonds to the DTB ureido carbonyl and the AdoMet 3′-hydroxyl group, while Asp155 forms hydrogen bonds to both the 2′- and 3′-hydroxyl groups of AdoMet (Figure 1). To investigate the role of these two highly conserved residues, Asn153 and Asp155 were substituted with other amino acids both individually and together. Four individual Asn153 mutant enzymes were generated, including Asn153Ala, Asn153Asp, Asn153Gln, and Asn153Ser. Four individual Asp155 mutant enzymes were generated, including Asp155Ala, Asp155Asn, Asp155Glu, and Asp155Ser. In addition, one mutant enzyme was generated that contained a double mutation, replacing both residues with alanine. All of the mutant proteins exhibited similar expression levels and purification elution profiles as those observed for WT enzyme. In addition, SDS−PAGE of the nine mutant enzymes showed a single band that resolved at the same position as WT enzyme (see Supporting Information), indicating each mutant was the same molecular weight and was not subject to significant proteolysis.

One measure of proper protein folding for this enzyme is through the detection of the presence of the [2Fe-2S]$^{2+}$ cluster in the aerobically purified protein. The active form of BioB contains two FeS clusters, a stable [2Fe-2S]$^{2+}$ cluster, and an air-sensitive [4Fe-4S]$^{2+}$ cluster (*15, 21*). The presence of these clusters is necessary for the high-affinity binding of both DTB and AdoMet (*22*). During aerobic purification of BioB, the [4Fe-4S]$^{2+}$ cluster is generally not retained and must be subsequently reconstituted under anaerobic conditions prior to binding or activity assays. However, if the purified protein is properly folded, it should retain the stable [2Fe-2S]$^{2+}$ cluster, even under aerobic conditions. When the [2Fe-2S]$^{2+}$ cluster is present, the

purified enzyme has a characteristic brown color, which all of the purified mutant enzymes exhibited. Furthermore, UV−visible spectra of all purified mutant enzymes showed peaks at 332 and 452 nm characteristic of the [2Fe-2S]$^{2+}$ cluster (*23, 24*) in *E. coli* BioB (see Supporting Information). To more precisely measure the iron and sulfide content of the aerobically purified mutant and WT proteins, analytical iron and sulfide analyses were conducted. Aerobically purified enzyme should theoretically contain one [2Fe-2S]$^{2+}$ cluster per monomer with a predicted ratio of 2 Fe and 2 S per BioB monomer. We found that WT enzyme has an average [Fe]:[BioB] ratio of 1.7 ± 0.05 and an average [S]:[BioB] ratio of 2.6 ± 0.07 (Figure 3A). The lower than expected [Fe]:[BioB] ratio could indicate the presence of some apoprotein in the purified WT enzyme. The higher than expected [S]:[BioB] ratio is likely due to the presence of cysteine persulfide sulfur derived from oxygen degradation of the [4Fe-4S]$^{2+}$ cluster during purification. The Asn153 mutants have an overall slightly lower [Fe]:[BioB] ratio as compared with the Asp155 mutants (1.2 ± 0.2 vs 1.7 ± 0.1, $p \leq 0.05$), suggesting that the Asn153 residue may have some minor influence on the *in vivo* FeS assembly process or the stability of the [2Fe-2S]$^{2+}$ cluster. Despite these slight variations, all of the mutant enzymes are capable of binding the [2Fe-2S]$^{2+}$ cluster at a level comparable to and with a UV−visible spectrum indistinguishable from WT enzyme, suggesting that the mutant proteins adopt a fold similar to that of WT enzyme.

Substrate Binding by the Mutant Enzymes. The prior study by Lotierzo et al. suggested that the Asn153Ala and Asp155Ala mutant proteins could bind substrates (as indicated by qualitative spectroscopic changes) but could not catalyze biotin or 5′-deoxyadenosine production (*12*). Based upon these data, we expected that some of our mutant proteins would be inactive, and we wanted to examine whether this inactivity was due to an extremely low affinity for substrates or whether it reflects other structural alterations within the intact enzyme active site. To examine the binding of DTB and AdoMet in the mutant proteins, each was reconstituted with $Fe^{2+/3+}$ and $S^{2−}$ in an anaerobic environment and incubated with a 4-fold excess of DTB and AdoMet. Free substrate was separated from bound substrate by filtration through a 10 kDa centrifugal concentrator under a nitrogen atmosphere. HPLC analysis with UV detection was used to determine the precise free and total substrate concentrations in the filtrate and retentate. WT enzyme showed an approximate binding stoichiometry of 0.8 ± 0.04 for both DTB and AdoMet (Figure 3B). Enzymes with a single mutation at either residue bound DTB with a stoichiometry that ranged from 0.5 to 0.9 and bound AdoMet with a stoichiometry that ranged from 0.4 to 1.0 (Figure 3B). The Asn153Ser, Asp155Asn, and Asp155Glu mutant enzymes bind both DTB and AdoMet with an affinity similar to that of WT enzyme. The most severely impaired mutant is the double mutant enzyme, Asn153Ala/Asp155Ala, which binds 0.5 equiv of DTB and 0.2 equiv of AdoMet under the conditions and concentrations used in this analysis. Thus, all of the mutant enzymes were capable of binding both DTB and AdoMet to a significant extent, suggesting that if Asn153 and Asp155 were only necessary for promoting substrate binding, the mutant proteins should be catalytically active.
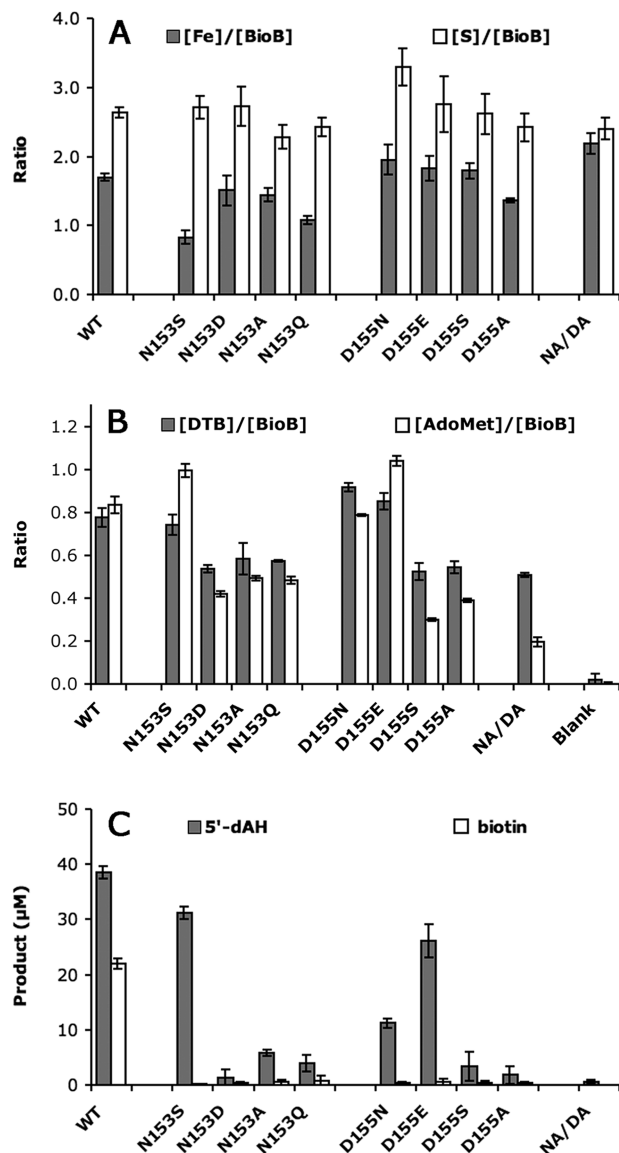
FIGURE 3: Binding and catalytic capabilities of the mutant enzymes. (A) Iron and sulfide content of the aerobically purified proteins. Iron analysis using bathophenanthroline and sulfide analysis using DMPD were performed as previously described (*15*). (B) Binding of DTB and AdoMet to the reconstituted proteins. BioB (100 μM) was reconstituted with Fe^{3+} (400 μM) and S^{2-} (400 μM) in DTT (5 mM) and Tris-HCl (50 mM) at pH 8.0 and incubated with DTB (200 μM) and AdoMet (200 μM). Free substrate was isolated by filtration using a 10 kDa centrifugal concentrator. HPLC analysis was used to determine the precise free and total substrate concentrations. (C) Catalytic activity of WT and mutant enzymes. Reconstituted BioB (50 μM) was incubated with DTB (200 μM) and AdoMet (500 μM) under our standard anaerobic assay conditions for 3 h at 37 °C. HPLC analysis with UV detection using external standards was used to determine the concentration of biotin (gradient I) and 5′-dAH (gradient II) in the final assay mixture.

The binding studies described above were conducted at a single set of substrate concentrations and thus represent a single data point that gives a rough estimate of relative substrate affinity. However, decreased binding levels could be caused by a number of factors, including decreased substrate affinity or incomplete saturation due to the potential presence of apoprotein or inactive conformations. To verify that the decrease in binding was dependent on substrate concentration and to provide a more quantitative understanding of the observed impaired substrate binding, we conducted
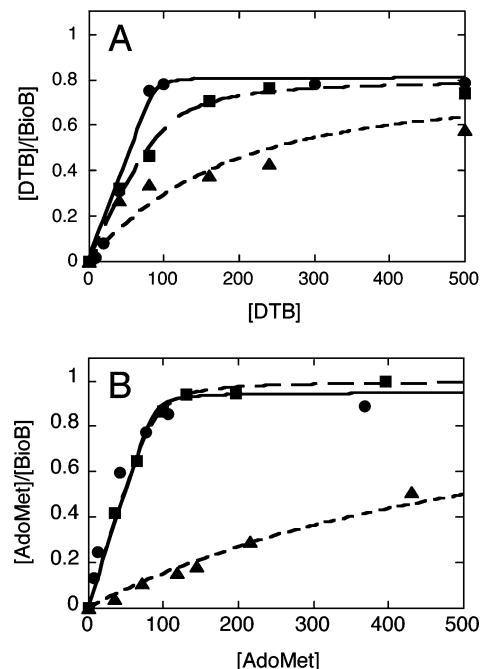

FIGURE 4: Binding of DTB and AdoMet to reconstituted WT (●), Asn153Ser (■), and Asn153Gln (▲) proteins. (A) Dethiobiotin (0−500 μM) and AdoMet (1 mM) were incubated with reconstituted protein (100 μM), and each sample was subjected to filtration and HPLC analysis as described for Figure 3B. Data are fit to a quadratic binding isotherm with 0.8 functional active site per monomer, yielding the following binding constants: WT, $K_d^{DTB} = 0.5 \pm 1$ μM; Asn153Ser, $K_d^{DTB} = 11 \pm 3$ μM; Asn153Gln, $K_d^{DTB} = 110 \pm 30$ μM. (B) AdoMet (0−500 μM) and DTB (1 mM) were incubated with reconstituted protein (100 μM), and each sample was subjected to filtration and HPLC analysis. Data are fit to a quadratic binding isotherm with 0.95 functional active site per monomer, yielding the following binding constants: WT, $K_d^{AdoMet} = 1.0 \pm 0.5$ μM; Asn153Ser, $K_d^{AdoMet} = 3.0 \pm 1.0$ μM; Asn153Gln, $K_d^{AdoMet} = 530 \pm 180$ μM.

detailed binding studies over a range of substrate concentrations using two selected mutants, Asn153Ser and Asn153Gln, that are representative of the mutant enzymes that exhibited moderate and low binding levels. To determine the affinity for DTB, the selected wild-type and mutant enzymes (100 μM) were reconstituted with $Fe^{2+/3+}$ and S^{2-} in an anaerobic environment and incubated with varying concentrations of DTB (0−500 μM) at a constant concentration of AdoMet (1 mM). Free unbound DTB was isolated from a mixture of free and bound DTB by filtration through a 10 kDa centrifugal concentrator. HPLC analysis (gradient I) was used to determine free and total DTB concentrations in the filtrate and retentate, and the resulting data were analyzed using a quadratic binding isotherm to provide the following dissociation constants: wild type, $K_d^{DTB} = 0.5 \pm 1$ μM; Asn153Ser, $K_d^{DTB} = 11 \pm 3$ μM; Asn153Gln, $K_d^{DTB} = 110 \pm 30$ μM (Figure 4A). In a similar manner, the affinity for AdoMet was examined by incubating wild-type and mutant proteins with varying concentrations of AdoMet (0−500 μM) and a constant concentration of DTB (1 mM). A small amount of the free unbound AdoMet was isolated from the mixture of free and bound AdoMet by filtration through a 10 kDa centrifugal concentrator. The free and total AdoMet concentrations were determined by an HPLC analysis optimized for AdoMet detection by incorporation of the ion-pairing reagent heptanesulfonic acid into the HPLC buffer

(gradient II). The resulting data were analyzed using a quadratic binding isotherm to provide the following dissociation constants: wild type, $K_d^{AdoMet} = 1.0 \pm 0.5\ \mu M$; Asn153Ser, $K_d^{AdoMet} = 3.0 \pm 1.0\ \mu M$; Asn153Gln, $K_d^{AdoMet} = 530 \pm 180\ \mu M$ (Figure 4B). Most importantly, both the DTB and AdoMet analyses indicate that decreased binding is due to a simple decrease in affinity. There is no evidence for complicating factors such as cooperativity or decreased saturation due to the presence of apoprotein or alternate impaired protein conformations.

The decrease in affinity can be analyzed in terms of a simple change in the free energy of substrate binding:

$$\Delta\Delta G^\circ binding = -RT \ln\left(\frac{K_d^{WT}}{K_d^{mutant}}\right) \qquad (1)$$

The decreased binding energy due to the Asn153Ser mutation is a relatively modest 0.65 kcal/mol for AdoMet and 1.8 kcal/mol for DTB. The decreased binding energy due to a more impaired mutation such as Asn153Gln is 3.7 kcal/mol for AdoMet and 3.2 kcal/mol for DTB. On the basis of this analysis and the relatively minor binding deficiencies shown in Figure 3B, we can conclude that Asn153 and Asp155 contribute relatively little energy for binding AdoMet and DTB. Our subsequent studies were therefore performed to examine whether these conserved residues might play a role in promoting or controlling the ensuing radical chemistry.

Catalysis by the Mutant Enzymes. The catalytic activity of wild-type and mutant enzymes was measured by incubating each protein (50 μM) with an excess of DTB (500 μM) and AdoMet (1 mM) under standard assay conditions for 3 h at 37 °C. HPLC analysis using external standards was used to determine the concentration of biotin (gradient 1) and 5′-dAH (gradient 2) in the final assay mixture. In agreement with the previous results of Lotierzo et al., we observe that none of the mutant enzymes produced a significant amount of biotin, less than 1 μM as compared with the 22 μM produced by WT enzyme (Figure 3C). While for most mutant enzymes biotin could not be observed by HPLC using UV detection (see Figure 5 for representative examples), there is in fact a trace amount of biotin being generated, as the correct mass for biotin is detected at the appropriate elution time by HPLC ESI MS analysis (see Supporting Information). Interestingly, while none of the mutants produce a significant amount of biotin, most are still able to catalyze reductive cleavage of AdoMet. The mutant enzymes that show the highest level of 5′-dAH production, Asn153Ser, Asp155Glu, and Asp155Asn, are the same mutants that show the highest level of substrate binding (Figure 3B,C). Taken together, these results suggest that the generation of 5′-dAH through reductive cleavage of the AdoMet sulfonium is not a particularly sensitive reaction and does not require that specific residues interact with the AdoMet ribose. However, the immediate product of reductive cleavage, the 5′-dA• radical, is a highly reactive oxidant, and the subsequent formation of 5′-dAH in the absence of biotin implies that alternate oxidized products must be formed. The identities of these alternate products may provide clues regarding the important role of Asn153 and Asp155 in guiding the reaction outcome.
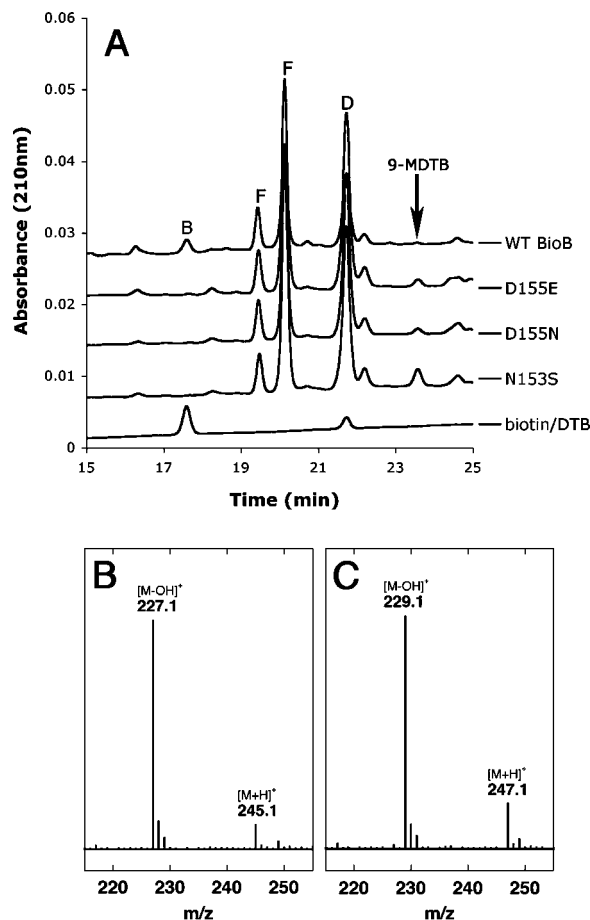

FIGURE 5: Formation of stoichiometric 9-mercaptodethiobiotin by the Asn153Ser mutant enzyme following a standard assay for 2 h at 37 °C. (A) HPLC analysis shows formation of a new stoichiometric product that elutes after DTB. This same product is detected at lower levels in most other mutants, including Asp155Glu and Asp155Asn shown here, and at much lower levels in WT enzyme. Abbreviations: B, biotin; D, DTB; F, flavin mononucleotide and riboflavin (from flavodoxin). (B) ESI MS analysis of biotin produced by WT enzyme and eluting at ∼17.5 min. Calculated [M + H]$^+$ = 245.10. (C) ESI MS analysis of 9-MDTB produced by the Asn153Ser mutant enzyme and eluting at ∼23.5 min. Calculated [M + H]$^+$ = 247.11. Assays were conducted as described in Figure 3C, and the HPLC analysis shown was conducted using gradient I with UV detection at 210 nm.

The Asn153Ser Mutant Enzyme Produces 9-Mercaptodethiobiotin as a Stoichiometric Product. The production of high levels of 5′-deoxyadenosine with no concomitant biotin formation by the Asn153Ser mutant enzyme (Figure 3C) suggested formation of an alternate product. To examine whether any alternate products derived from DTB were being formed, we conducted standard assays of each mutant for 2 h and analyzed the resulting soluble extract by HPLC, using conditions optimized for the analysis of biotin and DTB with UV detection at 210 nm. Several mutant enzymes catalyzed formation of a new product that elutes after DTB (Figure 5A). The level of this product was especially high in the reaction extract of the Asn153Ser mutant enzyme, with a concentration approaching that of biotin in the WT enzyme extract (Figure 5A). ESI MS analysis of the new peak eluting after the DTB peak in Asn153Ser mutant enzyme sample revealed a parent ion at [M + H]$^+$ = 247.1 (Figure 5C), 2 mass units higher than for the biotin peak in the WT enzyme sample ([M + H]$^+$ = 245.1, Figure 5B) and 32 mass units

higher than DTB (Supporting Information), corresponding to the addition of one sulfur to DTB to form either 6- or 9-mercaptodethiobiotin (MDTB). The incorporation of a sulfur atom into this new product is further demonstrated by the presence of a minor monoisotopic peak at a $[M + H]^+ = 249.1$ with ~5% relative abundance, which corresponds to the natural abundance of ^{34}S (4.2%). For mass spectra of biotin (Figure 5B), MDTB (Figure 5C), and DTB (Supporting Information), dehydration of the carboxylic acid during ionization also produces a dominant fragmentation peak at $[M - OH]^+$.

To confirm that the product formed by the Asn153Ser mutant enzyme was 9-MDTB, and not 6-MDTB, we examined the product formed from a sample of synthetic DTB that has three deuterium atoms incorporated into the C9 methyl group (*3, 13*). A similar characterization of the formation of 9-MDTB as an intermediate by the WT enzyme has been reported in detail elsewhere (*5*). The mass spectrum of ($^2H_3$-9-*methyl*)-DTB exhibited a parent ion peak at $[M + H]^+ = 218.2$, 3 mass units higher than unlabeled DTB, with $[M + H]^+ = 215.1$ (Supporting Information). If the first step in biotin formation involves abstraction of a hydrogen/deuterium atom from C9, then one deuterium should be transferred to 5′-dAH, and the intermediate/product formed from labeled DTB should retain only two deuterium atoms. We observed that the major peak in the mass spectrum of the product formed from ($^2H_3$-9-*methyl*)-DTB by the Asn153Ser mutant enzyme at $[M + H]^+ = 249.1$ is shifted by only +2 mass units from the unlabeled sample with $[M + H]^+ = 247.1$, indicating that the thiol has replaced a deuterium at the C9 position.

Kinetic Characterization of 9-MDTB Formation by the Asn153Ser Mutant Enzyme. To provide further evidence that the 9-MDTB is a stoichiometric abortive product of the Asn153Ser mutant enzyme, we compared the kinetics of formation of 9-MDTB to the production of biotin by WT enzyme. Following a short lag, biotin is initially produced by the WT enzyme at a rate of 0.05 ± 0.02 min^{-1}, while the production gradually slows after 45 min, perhaps due to binding of products to unreacted enzyme (Figure 6A, triangles). The Asn153Ser mutant produces 9-MDTB with no noticeable lag at an initial rate of 0.07 ± 0.02 min^{-1} and also slows slightly after 45 min (Figure 6A, circles). In addition, the formation of 9-MDTB shows a saturable dependence on both AdoMet and DTB (Figure 6B). Assuming a maximum product stoichiometry of 1:1 9-MDTB:BioB monomer at sufficiently high AdoMet and DTB concentrations, then we can estimate pseudo-Michaelis constants: $K_M^{AdoMet} = 500$ μM and $K_M^{DTB} = 305$ μM.[2] In both cases, these kinetic constants are ~100-fold higher than observed for biotin production by the WT enzyme (*25*).

Since the Asn153Ser mutant enzyme is capable of generating 9-MDTB at a rate comparable to WT enzyme (Figure 6A) and produces approximately 1 equiv of 5′-dAH per 9-MDTB, the failure to produce biotin suggests a defect
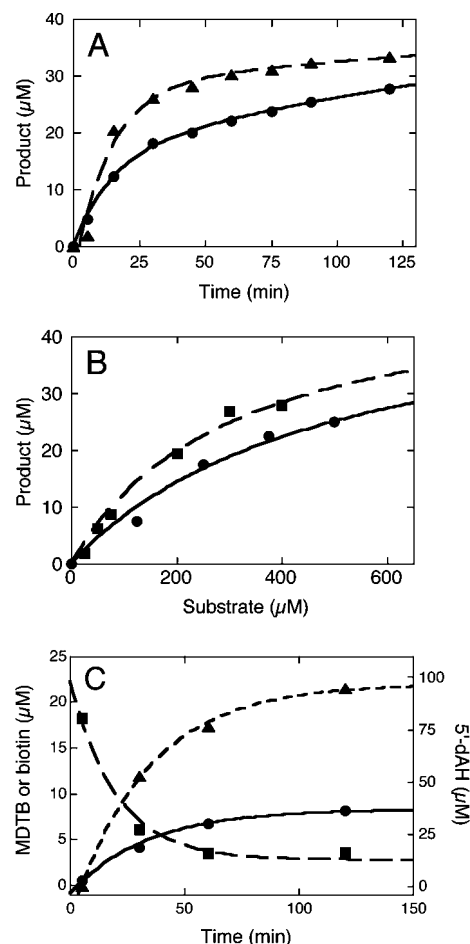
---

[2] Since BioB is a single-turnover enzyme that cannot undergo steady-state turnover, analysis of the data using Michaelis−Menten kinetics is not entirely appropriate, and the K_m values do not have the usual kinetic meaning. We have resorted to this simplistic analysis, however, because the observation of saturable kinetics implicates the involvement of a Michaelis enzyme−substrate complex in the generation of abortive product.

FIGURE 6: Kinetic characterization of 9-MDTB formation. (A) The Asn153Ser mutant enzyme (50 μM) produces 9-MDTB (▲) at a rate that is similar to the rate at which the WT enzyme produces biotin (●). Each data set is fit to a sum of two exponential phases. The rate constant for the initial formation of 9-MDTB by the Asn153Ser mutant enzyme (0.07 ± 0.02 min^{-1}) is similar to the modeled rate constant for formation of biotin by the WT enzyme (0.05 ± 0.02 min^{-1}). (B) The formation of 9-MDTB by the Asn153Ser mutant enzyme (50 μM) shows a saturable dependence on both AdoMet (●) and DTB (■). Data were fit to the Michaelis−Menten equation [2] assuming saturation would produce stoichiometric 9-MDTB (50 μM), yielding the following parameters: $K_M^{AdoMet} = 500$ μM and $K_M^{DTB} = 305$ μM. (C) 9-MDTB (■) initially produced by the Asn153Ser mutant enzyme can be converted to biotin (●) by WT enzyme, although approximately 10 equiv of 5′-dAH (▲) is generated for each equivalent of biotin produced. Asn153Ser mutant enzyme was used to produce 9-MDTB, which was then purified by HPLC. WT enzyme (50 μM) was assayed in the presence of 9-MDTB (20 μM) and AdoMet (1 mM), and the concentration of each component in the assay mixture was determined by quantitative HPLC analysis using gradient I with UV detection at 210 nm.

at a late stage in catalysis. We envision two likely scenarios: either the mutant enzyme does not cleave the second equivalent of AdoMet due to improper alignment with the C6 position of the 9-MDTB intermediate or else the 9-MDTB intermediate is not retained during the exchange of 5′-dAH and methionine for a second equivalent of AdoMet. To address this second possibility, we compared the ability of WT and Asn153Ser mutant enzyme to bind and retain 9-MDTB produced during the course of an assay. Following a 2 h activity assay, the unquenched assay mixture was filtered through a 10 kDa centrifugal concentrator under anaerobic conditions. The concentration of substrates, inter-

mediates, and products in the eluted small molecule fraction was compared to the total concentration prior to filtration by HPLC, and the difference in concentration is presumed to be due to tight binding of the intermediate to the enzyme. After a 2 h assay, WT enzyme (50 μM) produced ~0.1 equiv of 9-MDTB (5 μM) with approximately 50% tightly bound to the protein, while the remainder is found in solution, presumably due to slow dissociation during the assay (Supporting Information). In contrast, the Asn153Ser mutant enzyme (50 μM) produced ~0.5 equiv of 9-MDTB (25 μM) with less than 10% bound to the protein, while the remainder was found free in solution. We conclude that 9-MDTB is not significantly retained by the Asn153Ser mutant enzyme during dissociation of the first equivalent of 5′-dAH and methionine.

To further demonstrate that the 9-MDTB produced by the Asn153Ser mutant enzyme is the identical species generated and consumed as an intermediate by the WT enzyme, we examined whether 9-MDTB produced by the Asn153Ser mutant enzyme could be converted to biotin by the WT enzyme. We collected 9-MDTB produced during turnover of the Asn153Ser mutant by HPLC, concentrated the extract under vacuum, and then added this concentrate to an assay of WT enzyme that did not contain DTB. This reaction mixture was followed by HPLC to determine the concentration of biotin and 5′-dAH. Starting with ~18 μM 9-MDTB, the WT enzyme generated ~8 μM biotin (Figure 6C), while the fate of the remaining 9-MDTB is unknown (we are assuming here that 9-MDTB and biotin have identical extinction coefficients). The time course for the conversion of 9-MDTB to biotin is comparable to the rate of biotin production by the WT enzyme. To our surprise, the conversion of 9-MDTB to biotin was accompanied by the production of ~90 μM (10 equiv) 5′-dAH. Since only one additional hydrogen atom abstraction is necessary for closure of the thiophane ring (Figure 2), the additional 5′-dAH must be generated by abortive quenching of the 5′-dA• radical, perhaps via abstraction of the 9-MDTB thiol hydrogen. Free unbound 9-MDTB has been observed as a minor byproduct during prolonged turnover of the WT enzyme (*5, 26, 27*) and has been detected as a minor biotin vitamer in *Arabidopsis* (*28*), and the question arises as to whether this aberrant product can be rescued and converted either back to DTB or forward to biotin. These results indicate that while unbound 9-MDTB can be converted to biotin by intact WT enzyme, this process consumes an excessive amount of AdoMet and the WT enzyme is clearly not optimized for this process.

Production of 5′-dAH by the Asp155Glu Mutant Enzyme. The reductive cleavage of AdoMet results initially in the formation of an unstable 5′-dA•, which in the WT enzyme is quenched by abstraction of a hydrogen atom from DTB, leading to formation of 5′-dAH and 9-MDTB or biotin. However, several mutant enzymes produce significant levels of 5′-dAH without producing either 9-MDTB or biotin (Figure 3C). For example, the Asp155Glu mutant enzyme binds both AdoMet and DTB with high affinity and produces 5′-dAH at a rate comparable to the WT enzyme but does not produce either biotin or 9-MDTB. The newly introduced hydrogen atom must derive from a component of the assay mixture. We examined two possibilities: (i) the 5′-dA• is intercepted by a buffer component, most likely the reactive

thiol groups of dithiothreitol, or (ii) abstraction of a hydrogen atom from DTB may proceed normally, but the resulting DTB radical cannot react with the $[2Fe-2S]^{2+}$ cluster and form the C9−S bond due to steric restrictions induced by the mutation and the DTB radical is then released into solution. To examine these scenarios, an assay of the Asp155Glu mutant enzyme with unlabeled DTB was carried out in a buffer composed of 1:1 D_2O/H_2O and compared to a control in H_2O. Mass spectra of 5′-dAH produced in the two different buffers showed no differences, either in the intensity or in the distribution of peaks associated with 5′-dAH, yielding a parent ion at $[M + H]^+ = 252.1$ for both samples (Figure 7B). This indicates that the 5′-dA• radical is not quenched by abstracting a hydrogen atom from the solvent-exchangeable position in a component of the protein or buffer and, in particular, could not have derived from the solvent-exchangeable thiol group in dithiothreitol. If the 5′-dA• is indeed capable of abstracting a hydrogen atom from DTB, but then the DTB radical cannot further react to generate the C9−S bond, then this radical might be released into solution where it would be quenched by abstraction of a hydrogen atom from solvent component. However, mass spectra of DTB reisolated following an assay in 1:1 D_2O/H_2O also showed no incorporation of ^2H into DTB (Figure 7C). We conclude that the 5′-dA• produced by the Asp155Glu mutant enzyme is likely quenched by hydrogen atom abstraction from a nonexchangeable protein residue or from the AdoMet-derived methionine product, although further analysis would be needed to confirm this.

Production of 5′-Mercapto-5′-deoxyadenosine by the Asp155Asn Mutant Enzyme. When the assay products generated by each mutant enzyme were analyzed using an HPLC protocol optimized for the resolution of AdoMet-derived products (gradient II), a new stoichiometric product was detected that elutes immediately following 5′-dAH (Figure 7A, arrow). This new product is particularly prominent in assays of the Asp155Asn and Asn153Ala mutant enzymes, where it is generated in concentrations comparable to or larger than 5′-dAH. This new product absorbs strongly at 260 nm, suggesting it is likely derived from AdoMet and retains the adenine base. Mass spectra of the new product formed by the Asp155Asn mutant enzyme exhibited a parent ion at $[M + H]^+ = 284.1$, which corresponds exactly to introduction of a sulfur atom into 5′-dAH (Figure 7D). The presence of a single sulfur atom is also supported by the observation of a minor peak at $[M + H]^+ = 286.1$ due to the natural abundance of ^{34}S (4.2%). We conclude that this new product is likely 5′-mercapto-5′-deoxyadenosine (5′-MdAH). To determine the source of the sulfur atom, we conducted an experiment in which the $[4Fe-4S]^{2+}$ cluster was first reconstituted with (^{34}S)sulfide (93.8 atom %). We have previously demonstrated that the $[4Fe-4S]^{2+}$ cluster could be reconstituted with $^{57}Fe^{2+/3+}$ (*21*) or $^{34}S^{2-}$ (M. Dotson and J. Jarrett, unpublished data) without significant contamination of the $[2Fe-2S]^{2+}$ cluster. If the sulfur is derived from the $[2Fe-2S]^{2+}$ cluster or the protein, the mass of 5′-MdAH produced by the Asp155Asn mutant enzyme should have no mass shift. If the sulfur is derived from the $[4Fe-4S]^{2+}$, there should be a shift of +2 mass units. Mass spectra of the new product showed a marked increase at $[M + H]^+ = 286.1$, indicating incorporation of ^{34}S derived from the $[4Fe-4S]^{2+}$ cluster with 72% fidelity (Figure 7E). Retention of
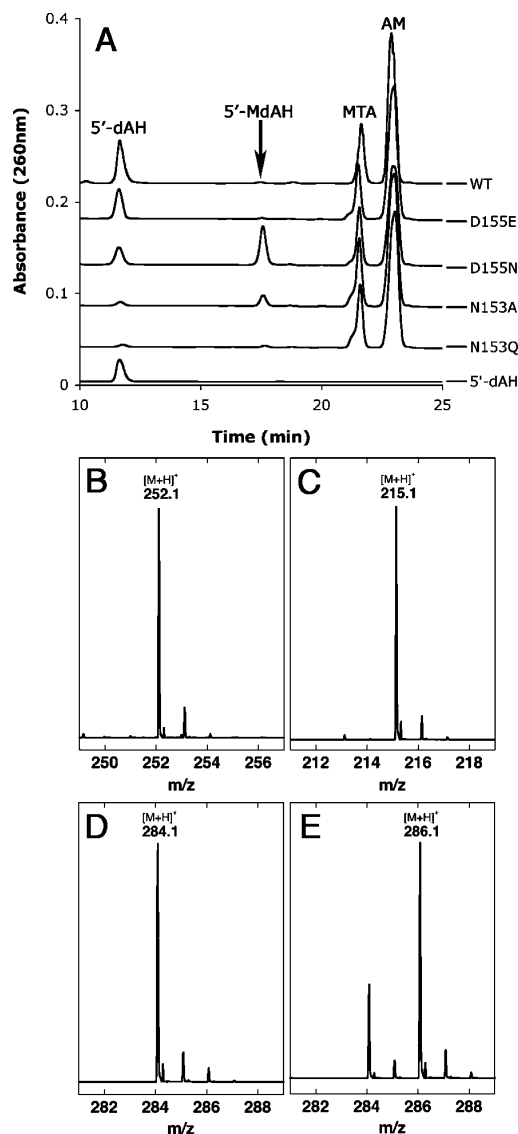
FIGURE 7: Production of 5′-dAH and 5′-mercapto-5′-deoxyadenosine by mutant enzymes. (A) HPLC analysis shows formation of 5′-dAH by the Asp155Glu mutant at a level comparable to the WT enzyme, in the absence of any detectable DTB-derived product. HPLC analysis also shows formation of a new stoichiometric product generated by the Asp155Asn mutant enzyme that elutes near 5′-dAH. A minor amount of the same product is observed in WT enzyme and those mutant enzymes that also produce 5′-dAH. Assays were conducted as described in Figure 3, and the HPLC analysis was conducted using gradient II with UV detection at 260 nm. Abbreviations: AM, AdoMet; MTA, 5′-methylthioadenosine. (B) ESI MS analysis of 5′-dAH produced by the Asp155Glu mutant enzyme in 1:1 D_2O/H_2O buffer demonstrates that the new hydrogen atom in 5′-dAH does not derive from an exchangeable position in the protein or buffer. Calculated $[M + H]^+ = 252.11$. (C) ESI MS analysis of DTB following incubation with the Asp155Glu mutant enzyme in 1:1 H_2O/D_2O buffer suggests that a DTB-derived radical is not released into solution, as this should have resulted in incorporation of deuterium from an exchangeable position in buffer. Calculated $[M + H]^+ = 215.14$. (D) ESI MS analysis of the new product formed by the Asp155Asn mutant enzyme gives an experimental $[M + H]^+ = 284.1$, which corresponds to introduction of sulfur (^{32}S: M = 31.972) into 5′-dAH (monoisotopic M = 251.103) yielding a calculated $[M + H^+] = 284.08$. The presence of a minor peak at $[M + H^+] = 286.1$ is due to the natural abundance of ^{34}S (4.22%). (E) ESI MS analysis of the new product produced from the Asp155Asn mutant enzyme in which the $[4Fe-4S]^{2+}$ cluster was reconstituted with $^{34}S^{2-}$ (93.8 atom %). An increase in the peak at $[M + H]^+ = 286.1$ indicates that 72% of the sulfur atoms in the new product are derived from the ^{34}S -labeled $[4Fe-4S]^{2+}$ cluster.

some ^{32}S in the product could be due to slow sulfide exchange between the $[4Fe-4S]^{2+}$ and $[2Fe-2S]^{2+}$ clusters during the prolonged assay incubation time or possibly to partial degradation of DTT present in large excess in the assay mixture. Interestingly, careful HPLC and ESI MS analysis indicates that 5′-MdAH is also present at ~1 − 2% in the WT enzyme reaction (Figure 7A), indicating that this is a naturally occurring side reaction for WT biotin synthase and perhaps also for other AdoMet radical enzymes.

DISCUSSION

Radical enzymes catalyze a diverse array of biochemical reactions (*29, 30*), such that it can seem at first glance that these reactions have little in common. However, all radical enzymes face some shared catalytic challenges. Each enzyme must generate a highly reactive radical, usually using a specially adapted metallocofactor, and must transfer that radical into the substrate via electron or hydrogen atom transfer. Each enzyme must then promote a highly specific reaction and ensure that at the end of the reaction the radical is quenched or transferred back to the cofactor and not released into solution. Perhaps most important for enzymes that generate and manipulate carbon radicals, each enzyme must prevent a number of possible side reactions with the protein or cofactor or with external buffer components. These potential side reactions include abstraction of a hydrogen atom from protein residues within the active site, alkylation of electron-rich protein residues or cofactors, or following release of the reactive radical into solution, abstraction of hydrogen atoms or alkylation of various cytosolic components including glutathione, nucleotides, RNA, or DNA.

Biotin synthase, in a mechanism presumably shared by all AdoMet radical enzymes, uses a $[4Fe-4S]^{2+}$ cluster to catalyze the reductive cleavage of the AdoMet sulfonium, generating a transient 5′-dA• radical. This carbon radical is highly reactive and can undergo a number of potential reactions. The structure of *E. coli* BioB suggests how the correct catalytic reaction is promoted: the 5′-methylene of AdoMet is in van der Waals contact with the C9 methyl of DTB ($d_{C-C} = 3.9$ Å) (*20*). This close proximity appears to be maintained by hydrogen bonds within the active site: the AdoMet ribose 2′- and 3′-hydroxyl groups form hydrogen bonds with Asp155 and Asn153, while the DTB ureido ring forms hydrogen bonds with Asn151, Asn153, and Asn222. With respect to AdoMet, Asp155 and Asn153 may also help to position the ribose and sulfonium in close proximity to the $[4Fe-4S]^{2+}$ cluster and could therefore also be important for the reductive cleavage of AdoMet and generation of the 5′-dA• radical. Of course, these residues could also be found in these specific positions within the active site simply because they can offer hydrogen bonds that promote binding of the substrates.

To reach a better understanding of the role of these hydrogen bonds between the AdoMet ribose and the protein, we changed Asn153 and Asp155 to residues that would either lengthen the side chain (Gln or Glu), shorten the side chain (Ser), or completely remove the side chain (Ala). We also explored whether Asn153 must be uncharged by mutating to Asp and whether Asp155 must be charged by mutating to Asn. We first examined whether Asp155 or Asn153 plays a significant role in binding either substrate to the enzyme.

An initial screen at a standard set of conditions demonstrated that all of the mutants could bind the substrates with relatively little impairment (Figure 3B). Even the double mutant Asn153Ala/Asp155Ala binds both substrates with a modest 2−4-fold decrease in stoichiometry. Translated into energetic terms in Figure 4, each mutation decreased the net binding energy by 0.5−3 kcal/mol, suggesting that these specific residues are not essential for binding the substrates and are not conserved solely for this purpose. Most likely, the majority of the binding affinity for AdoMet is provided by the hydrophobic adenine binding pocket on one end (*8*) and coordination of the methionyl carboxylate and amine to the $[4Fe-4S]^{2+}$ cluster (*31*) on the other end.

The reductive cleavage of the AdoMet sulfonium has been presumed to be a difficult reaction that requires a special arrangement of AdoMet with respect to the $[4Fe-4S]^{2+}$ cluster, and perhaps Asn153 and Asp155 are conserved to promote this catalytic structure. In a recent study by the Marquet group in which Asn153 and Asp155 were changed to Ala, they report that the resulting mutant proteins could not produce detectable levels of biotin nor could they catalyze the reductive cleavage of AdoMet (*12*). They conclude that the reductive cleavage of AdoMet is blocked in these mutants and suggest that removal of these hydrogen bonds in the active site could potentially have changed the redox properties of the clusters (*12*). In contrast with this hypothesis, we find that all of the mutant proteins can produce 5′-dAH using only the native flavodoxin reducing system, albeit at somewhat lower levels than the WT reaction. We would suggest that sulfonium reduction is not a particularly sensitive reaction and that Asn153 and Asp155 are not conserved in order to promote this reaction. However, it does appear to be important to have a hydrogen-bonding residue occupying at least one of these two positions within the active site. The double mutant Asn153Ala/Asp155Ala, despite binding both AdoMet and DTB, failed to produce significant amounts of 5′-dAH, perhaps because the missing residues allowed the sulfonium to be positioned too far from the $[4Fe-4S]^{2+}$ cluster. We conclude that the specific residues that hydrogen bond to the ribose are not significant in facilitating reductive cleavage, nor is the precise structural arrangement of the AdoMet, but perhaps only reasonably close proximity of AdoMet to the $[4Fe-4S]^{2+}$ cluster is necessary to promote electron transfer and reductive cleavage.

Perhaps not surprising was the finding that the reductive cleavage of AdoMet and the generation of 5′-dAH were not necessarily coupled to the formation of biotin nor any other detectable product. In particular, the Asp155Glu mutant appeared to cleave AdoMet and rapidly produce stoichiometric amounts of 5′-dAH without any production of a DTB-derived alternate product. Uncoupled cleavage of AdoMet has been reported as a side reaction for numerous AdoMet radical enzymes, particularly when sodium dithionite is used as an artificial reductant (*32*). Prior studies have demonstrated that WT BioB can produce several equivalents of 5′-dAH in the presence of excess AdoMet and dithionite (*33*), while 0.1−1 equivalent of uncoupled 5′-dAH production occurs during assay of BioB using the native flavodoxin reducing system (*5, 12*). This "uncoupled" cleavage reaction must in fact be coupled to the abstraction of a hydrogen atom from some unknown sacrificial donor. We were unsuccessful in identifying this donor but can conclude that 5′-dA• is not

released into solution, since this would almost certainly have been quenched by the large excess of dithiothreitol present in our assay buffers. In D_2O, this type of quenching should result in incorporation of deuterium into 5′-dAH, which we did not detect. Most likely, the Asp155Glu mutation reorients the 5′-dA• such that it cannot react with DTB and instead abstracts a hydrogen atom from a protein side chain or from the AdoMet-derived methionine within the active site. Future experiments should help to distinguish between these possibilities.

One other possible mode by which the 5′-dA• radical could be quenched within the active site is by alkylation of any nearby electron-rich species. Mutation of Asp155 to Asn produced a mutant enzyme that generated significant amounts of 5′-dAH, suggesting that uncoupled reductive cleavage of AdoMet was producing a 5′-dA• radical within the active site. However, upon careful characterization of the products produced by this mutant enzyme we detected a new AdoMet-derived product that eluted from the HPLC between 5′-dAH and 5′-methylthioadenosine (MTA). The mass spectrum of this product suggested that it corresponds to addition of sulfur to 5′-dAH, and the most logical conclusion is that attack of 5′-dA• on a sulfur donor has generated a new C−S bond and the product 5′-mercapto-5′-deoxyadenosine (5′-MdAH). This would occur through a mechanism similar to the proposed mechanism for incorporation of sulfur to generate biotin (Figure 2). We suspected that the sulfur donor in this case is the $[4Fe-4S]^{2+}$ cluster, and we selectively reconstituted this cluster with $^{34}S^{2-}$ in the Asp155Asn mutant enzyme. The labeled sulfur was incorporated into the 5′-MdAH product in ∼70% yield. Following these studies, we reexamined the reaction products generated by the other mutant and WT enzymes and found that 5′-MdAH is found in all of these samples. We propose that this is a common side reaction for all AdoMet radical enzymes and that each enzyme has likely evolved a restricted active site structure in part to avoid a reaction that not only consumes the substrate but also destroys the catalytic $[4Fe-4S]^{2+}$ cofactor.

AdoMet radical enzymes are most likely relatively "ancient" enzymes that have their beginnings in a world that was iron rich and oxygen poor. The facile production of 5′-dA• through reduction of the AdoMet sulfonium facilitates production of a powerful oxidant under anaerobic reducing conditions. However, production of a reactive intermediate that is also a potentially hazardous oxidant necessitates a high level of control to prevent irreversible damage to the enzyme or to other cellular components. In BioB, the position and trajectory of 5′-dA• is controlled at least in part by the highly conserved residues Asn153 and Asp155. Mutation of these residues leads to "active" enzymes that cannot couple radical generation and 5′-dAH production to formation of the correct product and instead make 5′-dAH, 5′-MdAH, and 9-MDTB in varying amounts. However, this study also demonstrates that even the wild-type enzyme is not able to completely control the radical chemistry, as 9-MDTB, 5′-MdAH, and a slight excess of 5′-dAH are always produced as minor byproducts during normal turnover. While it seems likely that radical enzymes would have evolved to minimize these adverse side reactions, evolution may have instead favored an enzyme that can contain unproductive radicals within the enzyme active site and thus protect the organism against self-inflicted free radical damage.

SUPPORTING INFORMATION AVAILABLE

SDS−polyacrylamide gel electrophoresis and UV−visible spectra of purified WT and mutant enzymes; additional mass spectra of unlabeled and ^{2}H-labeled dethiobiotin, 9-MDTB, and biotin produced by mutant enzymes; an analysis of 9-MDTB retention by WT and Asn153Ser mutant enzyme. This material is available free of charge via the Internet at http://pubs.acs.org.

REFERENCES

1. Jarrett, J. T. (2005) The novel structure and chemistry of iron-sulfur clusters in the adenosylmethionine-dependent radical enzyme biotin synthase. *Arch. Biochem. Biophys. 433*, 312–321.
2. Marquet, A., Tse Sum Bui, B., and Florentin, D. (2001) Biosynthesis of biotin and lipoic acid. *Vitam. Horm. 61*, 51–101.
3. Escalletes, F., Florentin, D., Tse Sum Bui, B., Lesage, D., and Marquet, A. (1999) Biotin synthase mechanism: evidence for hydrogen transfer from the substrate into deoxyadenosine. *J. Am. Chem. Soc. 121*, 3571–3578.
4. Ugulava, N. B., Sacanell, C. J., and Jarrett, J. T. (2001) Spectroscopic changes during a single turnover of biotin synthase: destruction of a [2Fe-2S] cluster accompanies sulfur insertion. *Biochemistry 40*, 8352–8358.
5. Taylor, A. M., Farrar, C. E., and Jarrett, J. T. (2008) 9-Mercaptodethiobiotin is formed as a competent catalytic intermediate by *Escherichia coli* biotin synthase. *Biochemistry 47*, 9309–9317.
6. Farrar, C. E., and Jarrett, J. T. (2007) Radical S-Adenosylmethionine (SAM) Superfamily, in *Encyclopedia of Life Sciences*, John Wiley & Sons, Chichester(http://www.els.net/[doi:10.1002/9780470015902.a0020547]).
7. Sofia, H. J., Chen, G., Hetzler, B. G., Reyes-Spindola, J. F., and Miller, N. E. (2001) Radical SAM, a novel protein superfamily linking unresolved steps in familiar biosynthetic pathways with radical mechanisms: functional characterization using new analysis and information visualization methods. *Nucleic Acids Res. 29*, 1097–1106.
8. Nicolet, Y., and Drennan, C. L. (2004) AdoMet radical proteins−from structure to evolution−alignment of divergent protein sequences reveals strong secondary structure element conservation. *Nucleic Acids Res. 32*, 4015–4025.
9. Layer, G., Moser, J., Heinz, D. W., Jahn, D., and Schubert, W. D. (2003) Crystal structure of coproporphyrinogen III oxidase reveals cofactor geometry of Radical SAM enzymes. *EMBO J. 22*, 6214–6224.
10. Hanzelmann, P., and Schindelin, H. (2004) Crystal structure of the *S*-adenosylmethionine-dependent enzyme MoaA and its implications for molybdenum cofactor deficiency in humans. *Proc. Natl. Acad. Sci. U.S.A. 101*, 12870–12875.
11. Lepore, B. W., Ruzicka, F. J., Frey, P. A., and Ringe, D. (2005) The x-ray crystal structure of lysine-2,3-aminomutase from *Clostridium subterminale*. *Proc. Natl. Acad. Sci. U.S.A. 102*, 13819–13824.
12. Lotierzo, M., Raux, E., Tse Sum Bui, B., Goasdoue, N., Libot, F., Florentin, D., Warren, M. J., and Marquet, A. (2006) Biotin synthase mechanism: mutagenesis of the YNHNLD conserved motif. *Biochemistry 45*, 12274–12281.
13. Marquet, A., Frappier, F., Guillerm, G., Azoulay, M., Florentin, D., and Tabet, J.-C. (1993) Biotin biosynthesis: synthesis and biological evaluation of the putative intermediate thiols. *J. Am. Chem. Soc. 115*, 2139–2145.
14. Ugulava, N. B., Gibney, B. R., and Jarrett, J. T. (2000) Iron-sulfur cluster interconversions in biotin synthase: dissociation and reassociation of iron during conversion of [2Fe-2S] to [4Fe-4S] clusters. *Biochemistry 39*, 5206–5214.
15. Ugulava, N. B., Gibney, B. R., and Jarrett, J. T. (2001) Biotin synthase contains two distinct iron-sulfur cluster binding sites: chemical and spectroelectrochemical analysis of iron-sulfur cluster interconversions. *Biochemistry 40*, 8343–8351.
16. Beinert, H. (1978) Micro methods for the quantitative determination of iron and copper in biological material. *Methods Enzymol. 54*, 435–445.
17. Fish, W. W. (1988) Rapid colorimetric micromethod for the quantitation of complexed iron in biological samples. *Methods Enzymol. 158*, 357–364.
18. Beinert, H. (1983) Semi-micro methods for analysis of labile sulfide and of labile sulfide plus sulfane sulfur in unusually stable iron-sulfur proteins. *Anal. Biochem. 131*, 373–378.
19. Broderick, J. B., Henshaw, T. F., Cheek, J., Wojtuszewski, K., Smith, S. R., Trojan, M. R., McGhan, R. M., Kopf, A., Kibbey, M., and Broderick, W. E. (2000) Pyruvate formate-lyase-activating enzyme: strictly anaerobic isolation yields active enzyme containing a [3Fe-4S]$^+$ cluster. *Biochem. Biophys. Res. Commun. 269*, 451–456.
20. Berkovitch, F., Nicolet, Y., Wan, J. T., Jarrett, J. T., and Drennan, C. L. (2004) Crystal structure of biotin synthase, an S-adenosylmethionine-dependent radical enzyme. *Science 303*, 76–79.
21. Ugulava, N. B., Surerus, K. K., and Jarrett, J. T. (2002) Evidence from Mossbauer spectroscopy for distinct [2Fe-2S]$^{2+}$ and [4Fe-4S]$^{2+}$ cluster binding sites in biotin synthase from *Escherichia coli*. *J. Am. Chem. Soc. 124*, 9050–9051.
22. Ugulava, N. B., Frederick, K. K., and Jarrett, J. T. (2003) Control of adenosylmethionine-dependent radical generation in biotin synthase: a kinetic and thermodynamic analysis of substrate binding to active and inactive forms of BioB. *Biochemistry 42*, 2708–2719.
23. Sanyal, I., Cohen, G., and Flint, D. H. (1994) Biotin synthase: purification, characterization as a [2Fe-2S] cluster protein, and in vitro activity of the *Escherichia coli* bioB gene product. *Biochemistry 33*, 3625–3631.
24. Duin, E. C., Lafferty, M. E., Crouse, B. R., Allen, R. M., Sanyal, I., Flint, D. H., and Johnson, M. K. (1997) [2Fe-2S] to [4Fe-4S] cluster conversion in *Escherichia coli* biotin synthase. *Biochemistry 36*, 11811–11820.
25. Sanyal, I., Gibson, K. J., and Flint, D. H. (1996) *Escherichia coli* biotin synthase: an investigation into the factors required for its activity and its sulfur donor. *Arch. Biochem. Biophys. 326*, 48–56.
26. Salib, A. G., Frappier, F., Guillerm, G., and Marquet, A. (1979) On the mechanism of conversion of dethiobiotin to biotin in *Escherichia coli*. III. Isolation of an intermediate in the biosynthesis of biotin from dethiobiotin. *Biochem. Biophys. Res. Commun. 88*, 312–319.
27. Shaw, N. M., Birch, O. M., Tinschert, A., Venetz, V., Dietrich, R., and Savoy, L. A. (1998) Biotin synthase from *Escherichia coli*: isolation of an enzyme-generated intermediate and stoichiometry of *S*-adenosylmethionine use. *Biochem. J. 330*, 1079–1085.
28. Baldet, P., Gerbling, H., Axiotis, S., and Douce, R. (1993) Biotin biosynthesis in higher plant cells. Identification of intermediates. *Eur. J. Biochem. 217*, 479–485.
29. Frey, P. A., Hegeman, A. D., and Reed, G. H. (2006) Free radical mechanisms in enzymology. *Chem. Rev. 106*, 3302–3316.
30. Stubbe, J., and van Der Donk, W. A. (1998) Protein radicals in enzyme catalysis. *Chem. Rev. 98*, 705–762.
31. Cosper, M. M., Jameson, G. N., Davydov, R., Eidsness, M. K., Hoffman, B. M., Huynh, B. H., and Johnson, M. K. (2002) The [4Fe-4S]$^{2+}$ cluster in reconstituted biotin synthase binds *S*-adenosyl-L-methionine. *J. Am. Chem. Soc. 124*, 14006–14007.
32. Jarrett, J. T. (2003) The generation of 5′-deoxyadenosyl radicals by adenosylmethionine-dependent radical enzymes. *Curr. Opin. Chem. Biol. 7*, 174–182.
33. Ollagnier-de Choudens, S., Sanakis, Y., Hewiston, K. S., Roach, P., and Munck, E. (2002) Reductive cleavage of S-adenosylmethionine by biotin synthase from *Escherichia coli*. *J. Biol. Chem. 277*, 13449–13454.